

Supporting Information

Small molecule BHJ solar cells based on DPP(TBFu)₂ and diphenylmethanofullerenes (DPM): Linking morphology, transport, recombination and crystallinity.

Daniel Fernández, Aurélien Viterisi, James William Ryan, Francesc Gispert-Guirado, Sara Vidal, Salvatore Filipone, Nazario Martín,* and Emilio Palomares*

Daniel Fernández, Aurélien Viterisi, James William Ryan and Emilio Palomares

Institute of Chemical Research of Catalonia (ICIQ). Avda. Països Catalans, 16. Tarragona. E-43007. Spain.

Francesc Gispert-Guirado

Universitat Rovira i Virgili. Avda. Països Catalans, XX. Tarragona. E-43007. Spain

*Sara Vidal, Salvatore Filipone, Nazario Martín**

Universidad Complutense de Madrid.

Email: nazmar@quim.ucm.es

Emilio Palomares*

ICREA. Passeig Lluís Companys, 32. Barcelona. E-08028. Spain

Email: epalomares@iciq.es

General:

DPP(TBFu)₂ was purchased from Lumtec Ltd. (Lumtec Ltd. Taiwan) and was used without further purification. DMP fullerenes derivatives were synthesised as described by Martin *et al.*¹ PC₇₀BM was purchased from Solenne (Solenne BV, the Netherlands). High purity (HPLC gradient grade, 99.9%) CHCl₃ was used for the active layer deposition. The solvent was dried with activated molecular sieves and kept in a sealed bottle with silver foil prior to use. Aluminium (99.999%) and LiF (99.995%) were purchased from Sigma-Aldrich.

Device Fabrication:

Pre-patterned Indium Tin Oxide (ITO) 5 Ohm/square (PSiOTec, Ltd., UK) sodalime glass substrates were first rinsed with acetone to remove the residual photoresist layer. The substrates were then placed in a teflon holder and sequentially sonicated in acetone (1 × 10 min) and isopropanol (2 × 10 min), and finally dried under a flow of Nitrogen. The ITO substrates were ozone-treated in a UV-ozone cleaner for 30 mins in ambient atmosphere, and subsequently coated in air with a layer of filtered (0.45 mm, cellulose acetate) solution of Poly(3,4-ethylenedioxythiophene) : poly(styrenesulfonate) (PEDOT:PSS, HC Starck Baytron P) (4500 rpm 30 seconds followed by 3500 rpm 30 seconds). The PEDOT:PSS film was dried at 120 °C under inert atmosphere for 15 min. Active layers were spin-coated (8000 rpm) in air over the PEDOT:PSS layer from a 20 mg/ml (total concentration) solution of DPP(TBFu)₂ and PC₇₁BM (6:4 w/w ratio). The approximate thickness of the active layer was 80 nm.

The solvent annealing step was carried out straight after deposition of the active layer by exposing the films to a saturated vapour of solvent in a closed vessel. The vessel (100 ml) was filled with 5 ml of CH₂Cl₂ and left sealed for 10 min. prior to the SVA step to ensure the atmosphere was saturated with solvent. The substrates were exposed to the solvent vapours from 15 seconds to several minutes by placing them in the solvent vessel.

The cathode layer was deposited by thermal evaporation in an ultra high vacuum chamber (1×10⁻⁶ mbar). Metals were evaporated through a shadow mask leading to devices with an area of 9 mm². LiF (0.6 nm) and Al (100 nm) were deposited at a rate of 0.1 Å/s and 0.5-1 Å/s respectively. Following fabrication, the films were maintained under a Nitrogen atmosphere and stored in the dark until used.

Device Characterization:

The UV-Vis absorption of films was measured using a Shimadzu UV-1700 spectrophotometer. The J-V characteristics of the devices were measured using a Sun 2000 Solar Simulator (150 W, ABET Technologies). The illumination intensity was measured to be 100 mW/cm^2 with a calibrated silicon photodiode (NREL). The appropriate filters were utilised to faithfully simulate the AM 1.5G spectrum. The applied potential and cell current were measured with a Keithley 2400 digital source meter. The current to voltage ($J-V$ curve) was plotted automatically with a home-built Labview© software. The IPCE (Incident Photon to Current conversion Efficiency) was measured using a home made set up consisting of a 150 W Oriel Xenon lamp, a motorized monochromator and a Keithley 2400 digital source meter. The photocurrent and irradiated light intensity were measured simultaneously and processed with a home-built Labview© software.

The thickness of the films was measured with a stylus profilometer Ambios Tech. XP-1, from a scratch made in the middle of the film.

Atomic Force Microscopy (AFM) of the samples was performed in tapping mode on a Molecular Imaging model Pico SPM II (pico +). Images were collected in air using silicon probes with a typical spring constant of 1–5 nN/m and at resonant frequency of 75 kHz.

X-ray diffraction characterisation

Conventional XRD measurements on thin films were carried out on a Bruker-AXS D8-Discover diffractometer with parallel incident beam (Göbel mirror), a vertical theta-theta goniometer, a XYZ motorized stage mounted on an Eulerian cradle, a incident and diffracted beam Soller slits, a 0.02° receiving slit and a scintillation counter as a detector. Diffraction pattern were recorded over an angular 2θ range of 1° to 8° . The data was collected with an angular step of 0.05° at 10 sec per step. $\text{CuK}\alpha$ radiation was obtained from a copper X-ray tube operated at 40 kV and 40 mA.

2D XRD measurements were performed with the same diffractometer equipped with an HI-STAR area detector (multiwire proportional counter of $30 \times 30 \text{ cm}$ with 1024×1024 pixel) and GADDS software (General Area Diffraction System). Samples were placed directly on the sample holder and the area of interest was selected with the aid of a video-laser focusing system. An X-ray collimator system allowed to analyse areas of $500 \mu\text{m}$ wide. 2D XRD

patterns (one frame) were collected covering $0.5^\circ 2\theta$ from at a distance of 30 cm from the sample. The exposition time was 600 sec per frame and it was chi-integrated to generate the conventional 2θ vs. intensity diffractogram.

Cyclic voltammetry

Cyclic voltamograms were recorded on a Autolab potentiostat.

The standard potentials were determined against Ferrocene as an internal standard and using $n\text{-Bu}_4\text{NPF}_6$ (0.1M) as supporting electrolyte. The standard potentials obtained for all fullerene derivatives are summarized in **Table 1S** and the Cyclic voltamograms are illustrated in **Figure 1S**, **Figure 2S** and **Figure 3S**.

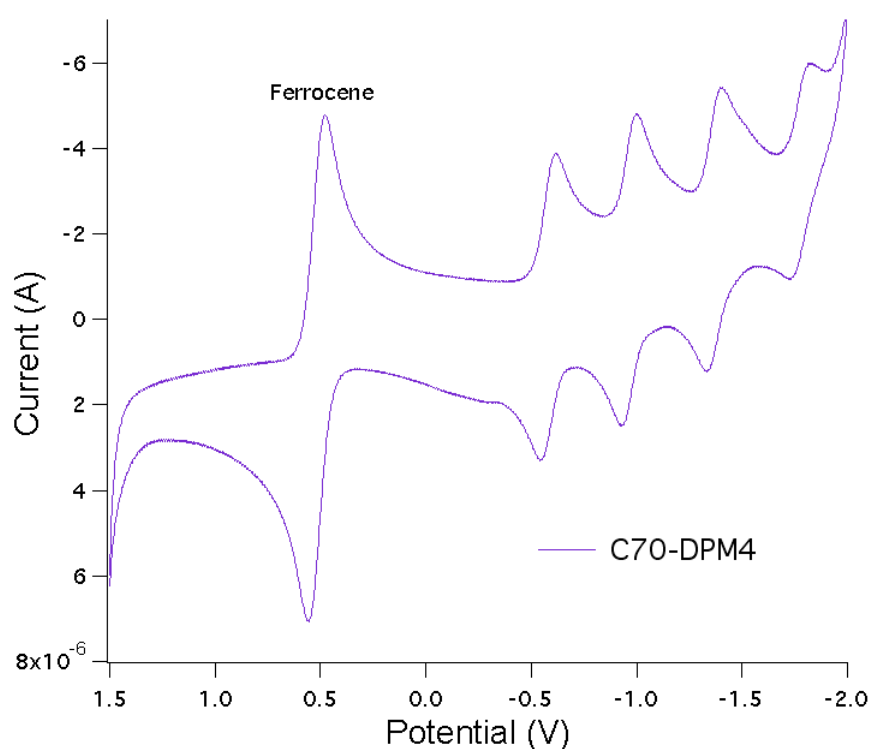


Figure 1S. Cyclic voltammetry of C70-DPM4

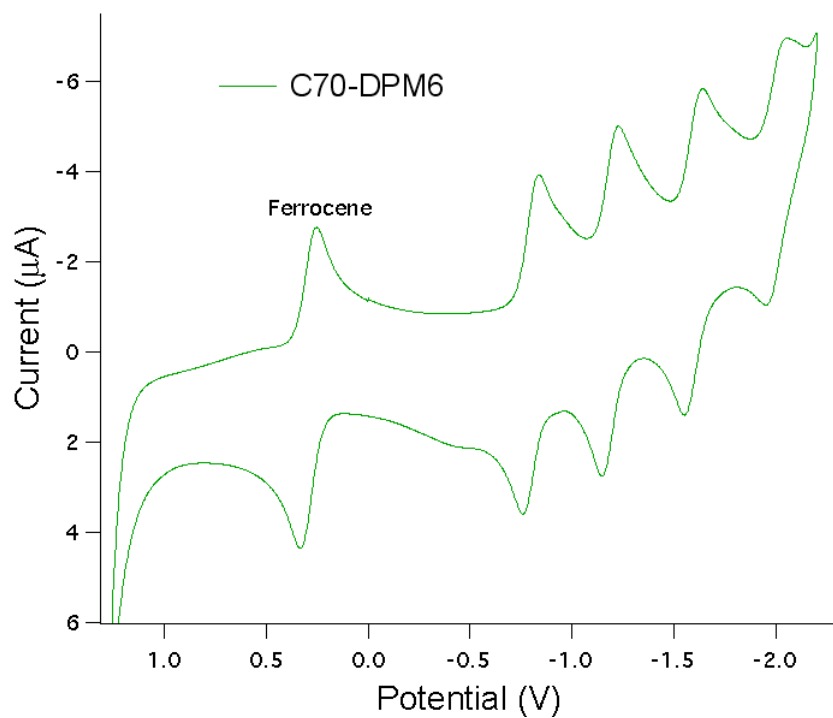


Figure 2S. Cyclic voltammetry of C70-DPM6

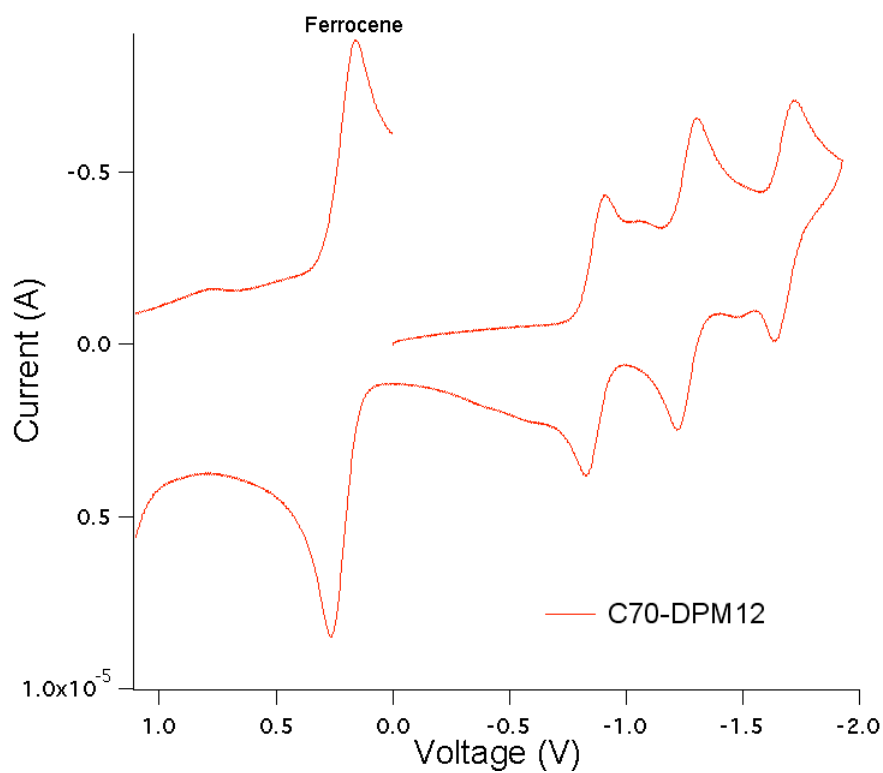


Figure 3S. Cyclic voltammetry of C70-DPM12

Table 1S. Electrochemical Redox potentials (V vs Fc/Fc⁺)

Fullerene	E ¹ _{red}	E ² _{red}	E ³ _{red}	E ⁴ _{red}
PC70BM	-1.09	-1.48	-1.88	-2.29
[70]DPM4	-1.09	-1.48	-1.89	-2.29
[70]DPM6	-1.09	-1.47	-1.89	-2.28
[70]DPM12	-1.09	-1.48	-1.89	-2.28

Hole and electron mobility

Mobility measurements were performed using hole or electron only devices. Hole-only devices had an ITO/PEDO:PSS/ DPP(TBFu)₂:Fullerene/Au architecture while electron-only devices had an ITO/ZnO/ DPP(TBFu)₂:Fullerene/Al structure (**Figure 4S**). Thicker metal cathodes (150nm) were used to aid in cooling to prevent damage associated with device heating when measuring at high voltages. Mobility values were obtained by fitting the obtained *J-V* plots in the SCLC region to a field dependent mobility as previously described,² as in equation (1) with the static permittivity of the active layer (ϵ) fixed to 3, γ being the field dependent parameter and μ_0 the zero-field mobility

$$J = \frac{5}{8} \frac{\epsilon \mu_0}{L^3} V^2 e^{0.897 \sqrt{|V|/L}} \quad \text{Equation (1S)}$$

Mobility measurements were repeated at least three times (using different devices) to confirm the reproducibility of the results. High electron mobility Zinc Oxide was deposited by a sol-gel technique as described in the literature.³

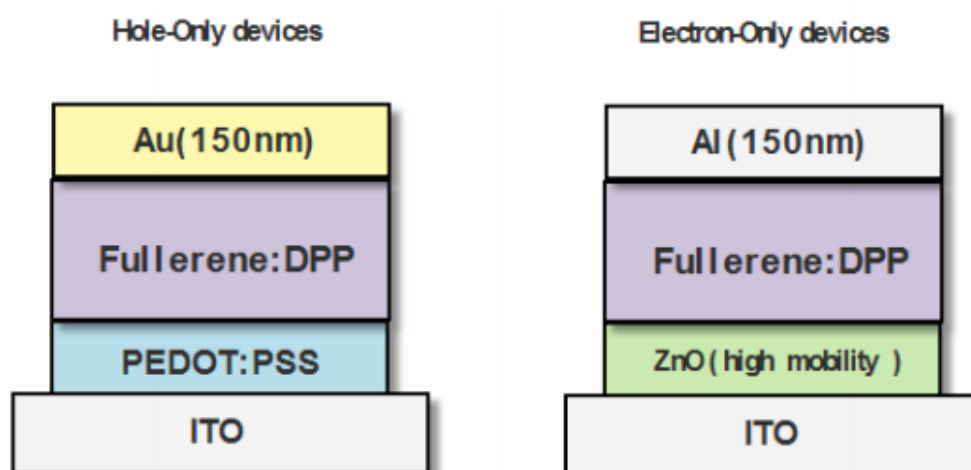


Figure 4S. Device architecture used for the different acceptors.

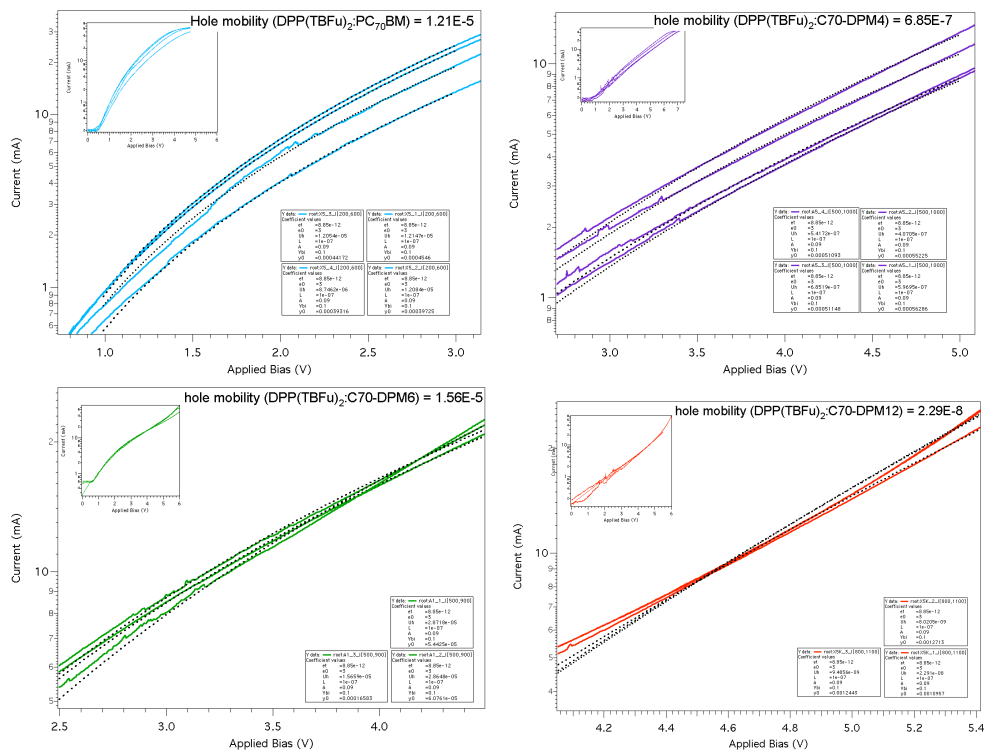


Figure 5S. Mott-Gurney plots of hole-only devices fabricated with DPP(TBFu)₂ and fullerene derivatives active layer blend. The plots were fitted to a field dependent mobility equation (equation (1S)). The graphs show the space charge limited region while the inset show the applied bias vs Current plot over the all range of applied bias.

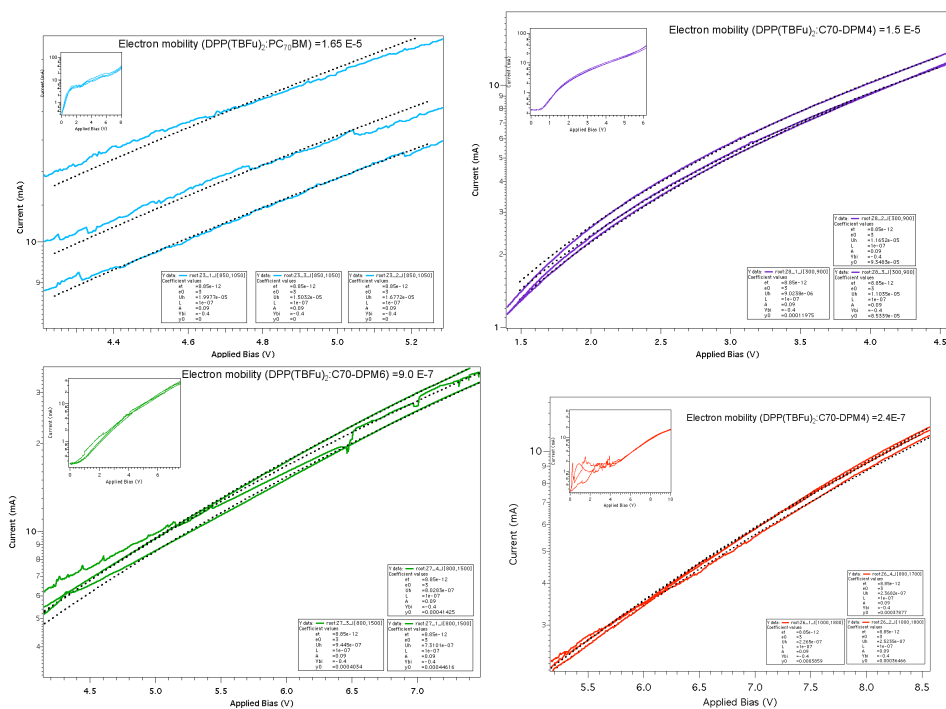


Figure 6S. Mott-Gurney plots of electron-only devices fabricated with DPP(TBFu)₂ and fullerene derivatives active layer blend. The plots were fitted to a field dependent mobility equation (equation (1S)). The graphs show the space charge limited region while the inset show the Applied bias vs Current plot over the all range of applied bias.

CE/TPV measurements

Transient photocurrent and transient photovoltage measurements were carried out as described by Durrant *et al.* using a similar set up. The charge losses due to recombination during the CE process were calculated through an iterative algorithm, described by Shuttle *et al.*⁴ and were found to be negligible in all measurements. The charge carrier density was corrected for the charge stored in the electrodes. To do so the experimental capacitance of all devices was measured by recording CE transients under negative bias in the dark and by fitting the Charge vs. Applied bias plot to a linear equation. The capacitance was found to vary from 2.5 nF to 3 nF.

The short circuit current vs light intensity was plotted in order to verify that these two variables vary linearly one respect to the other, thus indicating that non-geminate recombination processes are negligible under short circuit conditions ((**Figure 7S**))

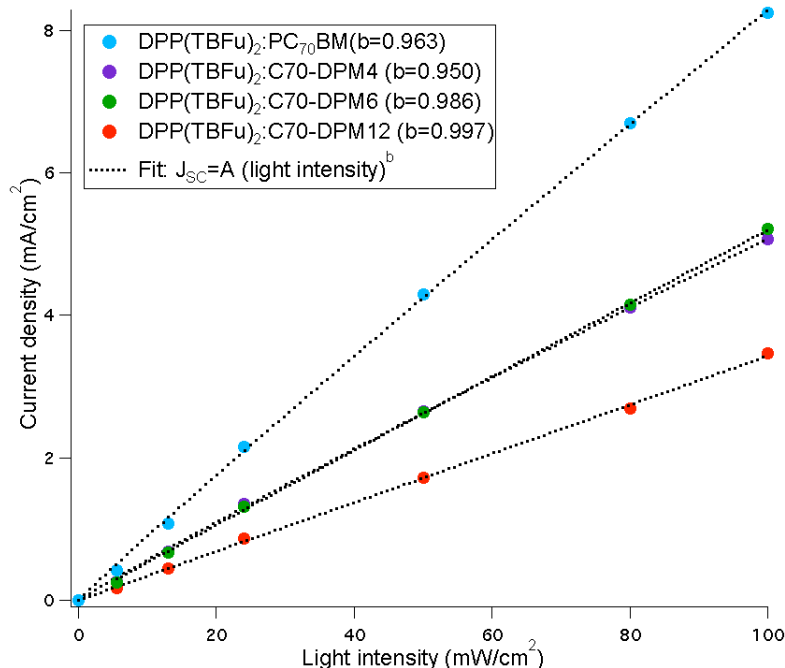


Figure 7S. J_{SC} vs Light intensity Plot. Curves are fitted to a power law.

Evidence for this process is provided in **Figure 8S** where the change in the UV-Vis absorption characteristics of DPP(TBFu)₂:C70-DPM12 active layer left at 40°C, in air was monitored over a week time and shows the appearance of the characteristic blue shifted bands assigned to the crystallisation of donor domains within hours.

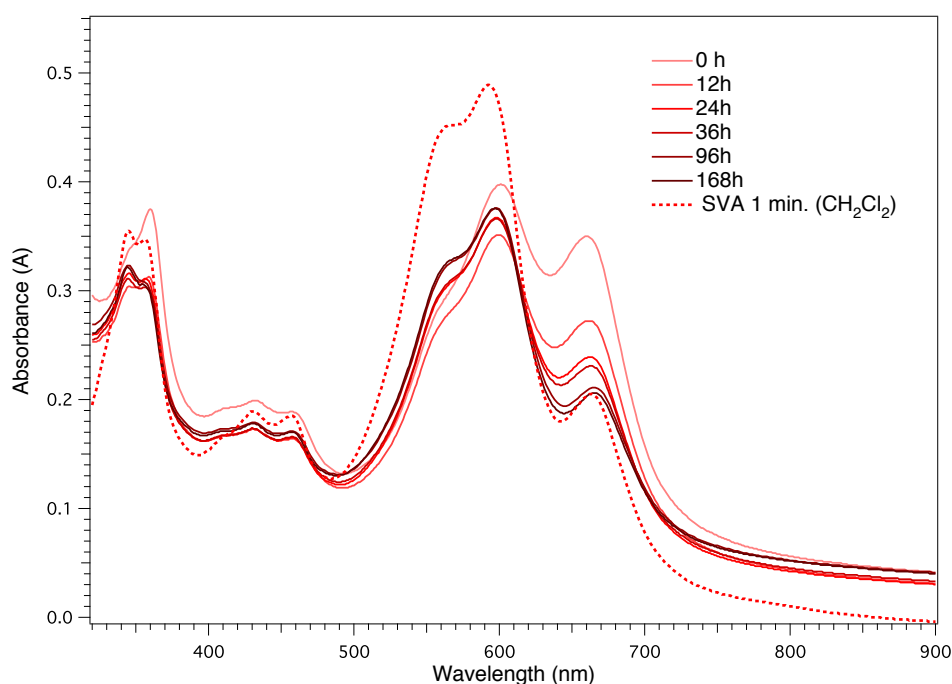


Figure 8S. UV-Vis spectra of initially un-annealed DPP(TBFu)₂:C70-DPM12 left in ambient air at 40°C recorded at different time intervals showing the self annealing process. The intensity of the original red shifted absorption band gradually decreases while the blue shifted band related to crystalline phase increases in intensity.

L-TAS spectrum for a 80nm thick DPP(TBFu)₂: PCB₇₀BM film

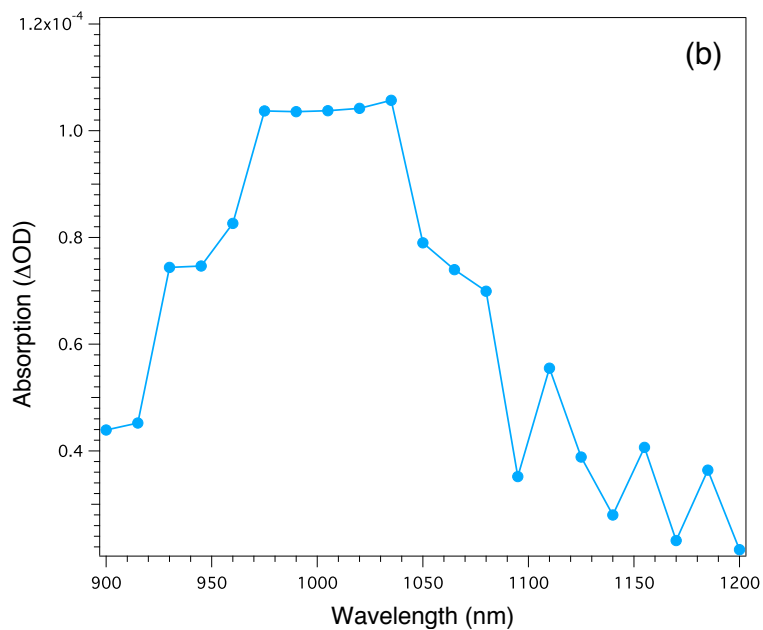


Figure 9S. L-TAS spectrum exciting at 580nm.

References

1. I. Riedel, E. von Hauff, J. Parisi, N. Martín, F. Giacalone and V. Dyakonov, *Adv. Funct. Mater.*, 2005, **15**, 1979.
2. a) J. M. Montero and J. Bisquert, *Solid-State Electron.*, 2011, **55**, 1; b) J. Bisquert, J. M. Montero, H. J. Bolink, E. M. Barea and G. Garcia-Belmonte, *phys. stat. sol. (a)*, 2006, **203**, 3762.
3. B. S. Ong, C. Li, Y. Li, Y. Wu and R. Loutfy, *J. Am. Chem. Soc.*, 2007, **129**, 2750.
4. C. G. Shuttle, PhD thesis, Imperial College London, 2008.